Protein Tuning of Excited-State Charge-Transfer Dynamics in Azurin

M. Adam Webb and Glen R. Loppnow*

Department of Chemistry, University of Alberta, Edmonton, Alberta, Canada T6G 2G2

Received: May 20, 1998; In Final Form: July 28, 1998

Resonance Raman spectra of azurin from *Alcaligenes denitrificans* have been measured at wavelengths throughout the S(Cys) → Cu charge-transfer absorption band to examine the effects of structure and environment on the excited-state charge-transfer dynamics. Measurement of the depolarization ratios suggest that the Raman scattering is enhanced by a single electronic transition. Self-consistent analysis of the absorption spectrum and the resonance Raman fundamental, overtone, and combination bands yields a total inner-sphere reorganization energy of 0.26 ± 0.02 eV, similar to that for *Pseudomonas aeruginosa*. The reorganization energy is distributed along similar vibrational modes in the two azurins, although the contribution from each mode is different. To understand these differences, molecular comparisons of the known structures and molecular modeling of the electrostatic field within the protein were performed. The results show that the two proteins have very similar structures, although the copper site itself has a slightly more tetrahedral geometry in *A. denitrificans*. The resonance Raman spectral differences between these two azurins are interpreted to arise from this copper site structural difference and a greater distribution of charges and/or dipoles near the coordinating histidines in *A. denitrificans*.

Introduction

Blue copper proteins are involved in electron transport processes in photosynthesis and respiration.[1,2] Azurin, a 14.6 kDa blue copper protein found in denitrifying bacteria, transports electrons from aromatic amine dehydrogenase to cytochrome *c* and/or nitrite reductase.[3−5] It has an unusual copper coordination geometry, a high reduction potential, and unusual spectral properties.[1,2,6] The copper ion cofactor of azurin adopts a distorted trigonal bipyramidal coordination geometry;[6] the copper sits slightly above the trigonal plane formed by two strongly bound histidines and a strongly bound cysteine and is weakly bound axially to a methionine S and glycine O (Scheme 1). The reduction potential is higher for azurin than aqueous Cu^{2+} (305 mV vs 115 mV).[1] The EPR spectrum of azurin shows an unusually narrow hyperfine splitting coupling[1], with $A_{||} = 0.0060$ cm^{-1}. The absorption spectra of azurins have a strong S → Cu charge-transfer transition at ∼620 nm which gives them their characteristic blue color. It appears that the unusual properties of the copper metal ion are due to the unique coordination geometry and protein environment.[1,2]

Resonance Raman spectroscopy is a sensitive probe of ground- and excited-state structure and dynamics. Previous resonance Raman studies of blue copper proteins have shown the ability of this technique to discriminate different ground-state active site structures in these proteins.[7−9] We have extended this work in our lab, by using resonance Raman intensities as a probe of the excited-state charge-transfer dynamics and the modulation of these ultrafast dynamics by the protein environment.[10−12] The exquisite sensitivity of the resonance Raman intensities to small changes in structure and environment, coupled with the well-characterized structures of these proteins, provides a sensitive probe of the factors which control charge transfer and electron transfer in these proteins.

In this work, we use resonance Raman intensities to measure the excited-state dynamics of azurin from *Alcaligenes denitrificans* (AD) and compare them to those in *Pseudomonas aeruginosa* (PA). The absorption spectrum and the resulting resonance Raman excitation profiles are analyzed using a self-consistent time-dependent wave packet propagation formalism. The total inner-sphere reorganization energy is found to be the same (0.26 ± 0.02 eV) for both species and distributed along similar vibrational modes, although the contribution from each mode is different for the two species. Correlation of the experimentally determined structures with the observed spectroscopic differences suggests that small differences in the protein can affect the excited-state dynamics through both structural and electrostatic mechanisms.

SCHEME 1

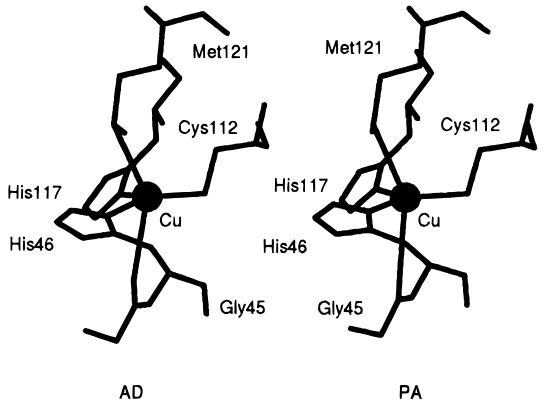

Experimental Section

Azurin from *A. denitrificans* was isolated and purified by methods described previously.[12] Column chromatography was used to obtain a purity ratio $A_{280}/A_{625} \leq 3.7$ (literature value[13] 3.6). A yield of 46−58 mg azurin per 100 g of cell paste was obtained. Azurin from *P. aeruginosa* was isolated and purified by methods described previously.[12]

Resonance Raman Spectroscopy. Samples for the resonance Raman experiments were prepared by quantitative dilution of azurin with either a cacodylate buffer solution (0.5−1.0 M

10.1021/jp982316n CCC: $15.00
Published on Web 10/10/1998

cacodylic acid, 0.01 M Tris−HCl, pH 8.7) or a nitrate buffer solution (1.0 M potassium nitrate, 0.01 M Tris−HCl, pH 8.7). Room-temperature resonance Raman spectra of azurin were obtained with 300 μL aqueous sample solutions (0.01 M Tris−HCl buffer, either 0.25−0.84 M cacodylic acid or 0.9 M nitrate, pH 8.7) having an absorbance of 1.9−5.9 OD/cm at 619 nm ($\epsilon_{619} = 5200$ M^{-1} cm^{-1}). The addition of cacodylate/cacodylic acid buffer did not have a noticeable effect on the absorption or resonance Raman spectra of azurin. Resonance Raman spectra were collected using a single monochromator with a CCD detector.[10,12] Frequencies are accurate to ± 2 cm^{-1}. Absorption spectra were recorded on a diode array spectrophotometer (Hewlett-Packard, Sunnyvale, CA, model 8452A). Measurement of the resonance Raman spectra and determination of the intensities were repeated on 3−6 fresh samples of azurin for each wavelength.

Analysis of the data was performed as previously described.[10,12] Bleaching of the sample was accounted for by measuring the absorbance at 580 nm ($\epsilon_{580} = 3562$ M^{-1} cm^{-1}) before and after each scan. The average absorbance was used to determine the concentration of azurin.

Absolute Raman cross-sections of cacodylate and nitrate were calculated from the *A*-term expression.[10,14,15] The calculated Raman cross-sections for cacodylate are 168, 126, 123, 106, 95.7, 88.2, 68.8, and 56.6 $\times 10^{-14}$ Å^2/molecule at 530.9, 565, 568.2, 588, 601, 612, 647.1, and 676.4 nm, respectively. The calculated Raman cross-sections for nitrate are 6.40, 5.73, 4.55, and 3.40 $\times 10^{-13}$ Å^2/molecule at 568.2, 581, 609, and 647.1 nm, respectively.

Depolarization ratios were measured using excitation wavelengths of 568.2, 581, 612, and 647.1 nm. The spectrum was measured with the polarizer set at 0° ($I_{||}$) and then with the polarizer at 90° ($I_\perp$) at each wavelength. The depolarization ratio is equal to the ratio of the intensities ($I_{||}/I_\perp$) for each band. The position of the polarizer was determined using the 459.7 cm^{-1} mode of CCl_4 which has a depolarization ratio of 0.02.[16] The 0° ($I_{||}$) position of the polarizer is determined by a minimum in intensity and the 90° ($I_\perp$) position by a maximum intensity of this band. Cacodylate was added as a check on the accuracy of the depolarization ratio. Its depolarization ratio was found to be 0.14 ± 0.08, which agrees with the literature value[10] of 0.18.

Intensity Analysis. The resonance Raman and absorption cross-sections in the Condon approximation can be written using the time dependent equations of Lee and Heller[10,17,18]

$$\sigma_R = \frac{8\pi E_S^3 E_L e^4 M^4}{9\hbar^6 c^4} \int_{-\infty}^{\infty} H(E_0)\, dE_0 \times \left| \int_0^{\infty} \langle f|i(t)\rangle\, e^{i(E_L + \epsilon_i)/\hbar}\, G(t)\, dt \right|^2 \quad (1)$$

$$\sigma_A = \frac{4\pi e^2 M^2 E_L}{6\hbar^2 cn} \int_{-\infty}^{\infty} H(E_0)\, dE_0 \times \int_{-\infty}^{\infty} \langle i|i(t)\rangle\, e^{i(E_L + \epsilon_i)/\hbar}\, G(t)\, dt \quad (2)$$

where E_L and E_S are the energies of the incident and scattered photons, M is the transition length, n is the refractive index, $H(E_0) = (1/\theta(2\pi)^{1/2}) \exp[-(E_0 - \bar{E}_0)^2/2\theta^2]$ is a normalized Gaussian distribution of site electronic energies centered at a mean 0−0 energy ($\bar{E}_0$ and having a width of θ, ϵ_i is the energy of the initial vibrational state, $G(t)$ is a decay function, $|i\rangle$ and $|f\rangle$ are the initial and final vibrational wave functions in the resonance Raman process, and $|i(t)\rangle = e^{-iHt/\hbar}|i\rangle$ is the initial ground-state vibrational wave function propagated on the excited-state potential surface. Significantly, the $\langle i|i(t)\rangle$ and $\langle f|i(t)\rangle$ overlaps are only sensitive to Δ, the difference in ground- and excited-state equilibrium geometries along each normal mode, within the separable harmonic oscillator approximation. Thus, the resonance Raman intensities directly reflect the dynamics of the excited state. The implementation of these equations has been described in detail.[10,11,15,17] Self-consistent analysis of the absorption spectrum and the resonance Raman excitation profiles was done in the same manner as previously described for plastocyanin[10,11] and azurin.[12]

Molecular Modeling. The structures of the proteins were obtained from the Brookhaven protein data bank[19] (5azu[20] and 2aza[6] for PA and AD, respectively) and compared by calculating the Cartesian root mean square (RMS) deviation:

$$\text{Cartesian RMS} = [\Sigma(\Delta X^2 + \Delta Y^2 + \Delta Z^2)/N]^{1/2} \quad (3)$$

where the sum is carried over all N atoms (hydrogen atoms were not included). The Brookhaven files contain more than one molecule of azurin per unit cell. For the RMS calculations and Cu−C_α distances, the A structure was selected; no significant differences were found by using other structures. All other distances and angles are averages of the reported X-ray structures for each azurin. The RMS per residue was calculated by neglecting the side chains of the amino acids as they are different for many residues; the two proteins have 48 different amino acids and a resulting homology of 63%. The two structures were then spatially overlapped using the remaining backbone structure and the copper metal, minimizing the overall RMS (1026 atoms, RMS = 0.827). The RMS for each residue was then calculated separately using only its backbone atoms (N, C_α, C, and O). These residue RMS values were then compared as a function of distance from the copper ion, using the C_α−Cu distance.

Results

The resonance Raman spectra of AD azurin were measured using excitation wavelengths throughout the S(Cys) → Cu absorption band. Figure 1 shows the resonance Raman spectrum taken at an excitation wavelength of 568.2 nm. The spectra at other wavelengths have similar relative intensities, indicating resonance enhancement occurs from a single electronic state. No reproducible peaks were observed at frequencies of less than 200 cm^{-1} because the single monochromator used to obtain the spectra was unable to separate the Rayleigh scattering from the low-frequency Raman signal. The cacodylate intensity standard appears at 605 and 638 cm^{-1}, marked with single asterisks in the figure. The intense bands between 300 and 500 cm^{-1} have been previously assigned to normal modes involving the Cu−S stretch mixed with other internal coordinates.[21−24] However, the exact assignments are still controversial.[21] The bands at 212, 251, and 274 cm^{-1} have been assigned to modes involving the Cu−N stretches.[21] The broad band at about 830 cm^{-1}, marked by double asterisks in the figure, is due to combination and overtone bands of the vibrations between 300 and 500 cm^{-1}. There is also a contribution at 825 cm^{-1} from the As=O stretch of cacodylate.[25,26]

The depolarization ratio of AD azurin was measured at 568.2, 581, 612, and 647.1 nm in order to determine if there is only one electronic transition which gives resonance enhancement. Figure 1 shows the parallel and perpendicular polarized spectra taken at an excitation wavelength of 568.2 nm; spectra at other wavelengths are similar. The relative intensities of the peaks do not change when different polarization components are detected, indicating that the depolarization ratio is the same for

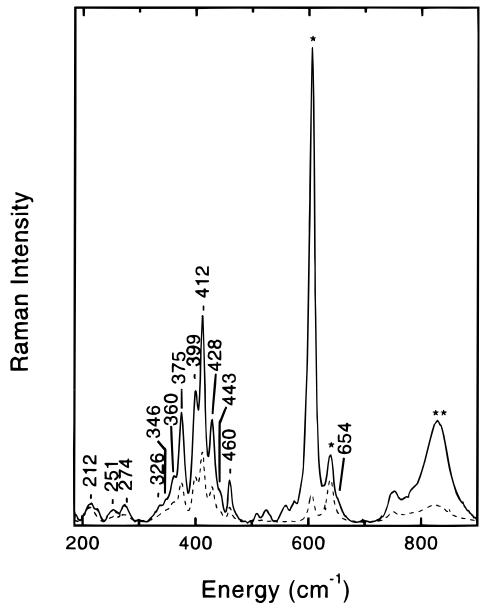

Figure 1. Resonance Raman spectra of *A. denitrificans* azurin polarized parallel (- - -) and perpendicular (—) at an excitation wavelength of 568.2 nm. The spectrum is the sum of two scans. The fundamental vibrations between 200 and 500 cm^{-1}, and the shoulder at 654 cm^{-1} were used in the analysis. Raman scattering of the internal intensity standard (cacodylate) is observed at 608 and 638 cm^{-1} (*). The broad band at ~820 cm^{-1} and the narrower band at ~750 cm^{-1} (**) are composed of the overtone and combination bands of the vibrations between 350 and 500 cm^{-1} and a cacodylate peak at 825 cm^{-1}.

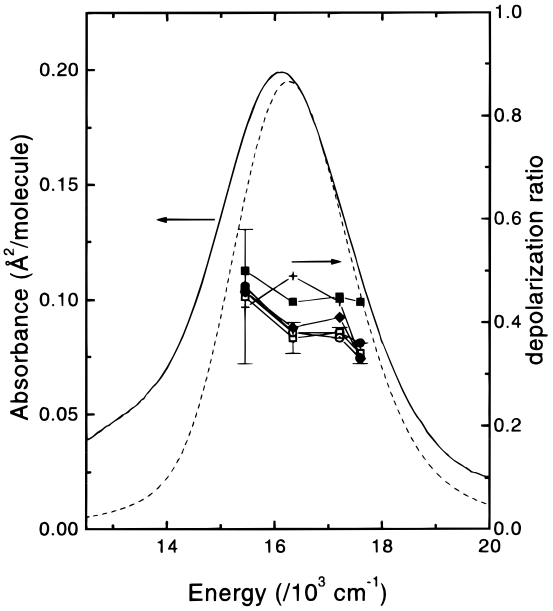

Figure 2. Experimental (solid line) and calculated (dashed lines) absorption spectra of *A. denitrificans* azurin (scale on left side). Deviations of the experimental absorption spectrum from the calculated absorption spectrum at both higher and lower energies are due to the presence of other charge-transfer and ligand field transitions which were not modeled and apparently contribute no resonance enhancement to the observed normal modes. Points are the depolarization measurements of azurin using four excitation wavelengths (scale on right side) for the most intense vibrational modes. The legend is as follows: ■ = 360 cm^{-1}, ● = 375 cm^{-1}, □ = 399 cm^{-1}, ○ = 412 cm^{-1}, ◆ = 428 cm^{-1}, + = 460 cm^{-1}). The error in the depolarization ratios are 0.02, 0.01, 0.03 and 0.13 at 568.2, 581, 612, and 647.1 nm, respectively. Representative error bars are indicated for the 399 cm^{-1} mode.

all modes. The depolarization ratio averaged over all modes at the four wavelengths was measured to be 0.41 ± 0.05. Figure 2 shows the measured depolarization ratios as a function of excitation wavelength for the strongest peaks. Within experimental error, the depolarization ratio of each band remains constant as the excitation wavelength is tuned throughout the absorption band. Additionally, the depolarization ratios of different bands are the same within experimental error. The slight increase in the depolarization ratios at 647.1 nm are probably due to a lower spectral signal-to-noise ratio at this wavelength, although it may also indicate that a second electronic transition is contributing to resonance enhancement of the Raman modes at this wavelength.

Figure 2 shows the experimental and calculated absorption spectra. Figure 3 shows the good agreement of the experimental and calculated resonance Raman excitation profiles. The parameters used for the calculated curves are given in Table 1. Deviations of the experimental absorption spectrum from the calculated spectrum at both higher and lower energies are due to the presence of other charge-transfer and ligand field transitions[27] which were not modeled and apparently contribute little or no resonance enhancement to the observed normal modes. Due to the presence of more than one electronic transition within the charge-transfer absorption band, the resonance Raman excitation profiles provided the primary constraints on the simulated spectral band shape, position, and bandwidth. Thus, scaling of the Δ values was determined by the width of the resonance Raman excitation profiles. Partitioning of the broadening into homogeneous and inhomogeneous components was primarily determined by the intensity of the resonance Raman excitation profiles.

The overtone and combination bands of AD azurin were measured at excitation wavelengths of 568.2, 581, 609, and 647.1 nm using nitrate as the internal standard, as a check on the self-consistency of the resonance Raman analysis and to test the presence of Duschinsky rotation.[28,29] Figure 4 shows the spectrum at an excitation wavelength of 568.2 nm. The spectra at other wavelengths exhibit similar spectral frequencies and intensities. The nitrate band appears at 1049 cm^{-1} and a small peak between 900 and 1000 cm^{-1} is a detector artifact.

TABLE 1: Mode-Specific Reorganization Energies of Azurin

azurin (AD)[a]			azurin (PA)[b]		
$\Delta\nu/cm^{-1}$	$\lvert\Delta\rvert$[c]	λ/cm^{-1}	$\Delta\nu/cm^{-1}$	$\lvert\Delta\rvert$[c]	λ/cm^{-1}
212	1.24	160	216	0.85	78
251	0.69	60	263	1.30	220
274	1.18	190			
326	0.43	30			
346	0.93	150	344	0.75	100
360	0.60	65			
375	1.26	300	371	1.60	470
399	1.30	340	401	1.20	290
412	1.28	340	408	1.60	520
428	1.09	250	426	1.30	360
443	0.43	40	439	0.23	12
460	0.58	80	454	0.31	22
			476	0.27	17
			493	0.13	4
654	0.22	16	654	0.18	11
total	2020 cm^{-1}			2100 cm^{-1}	

[a] Values for AD azurin from this work. Other parameters were the following: zero−zero energy, $E_0 = 14\,300$ cm^{-1}; transition length, $M = 0.73$ Å; temperature, $T = 0$ K; refractive index, $n = 1.33$; Lorentzian homogeneous line width, $\Gamma_L = 450$ cm^{-1}; Gaussian homogeneous line width, $\Gamma_G = 75$ cm^{-1}; inhomogeneous line width, $\Theta = 150$ cm^{-1}. [b] Values for PA azurin are from ref 12. [c] Δ values are in dimensionless normal coordinates. The reorganization energy in a particular mode, λ_i, is related to Δ_i by $\lambda_i = (\Delta_i^2\omega_i)/2$ where ω_i is the frequency in cm^{-1}.

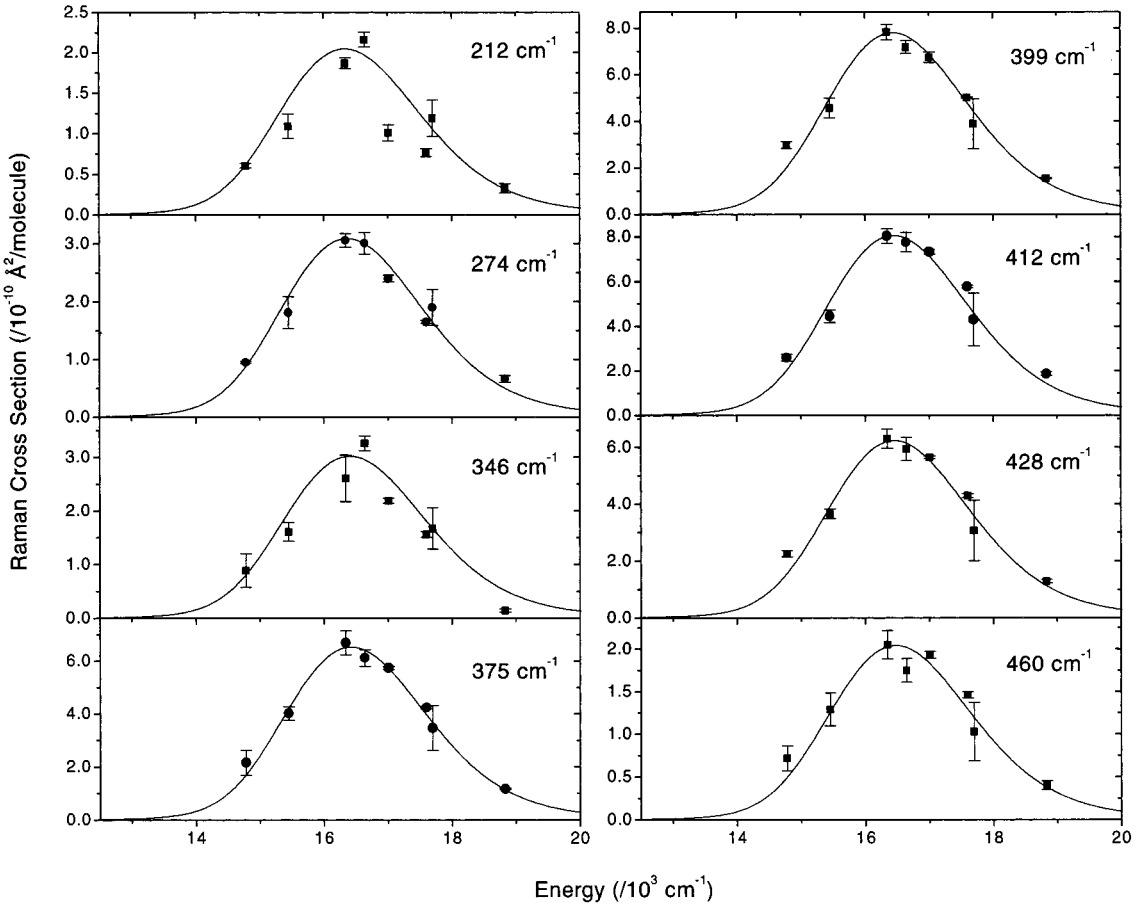

Figure 3. Experimental (points) and calculated (solid line) resonance Raman excitation profiles of *A. denitrificans* azurin. The excitation profiles were calculated with eq 1 using the parameters in Table 1.

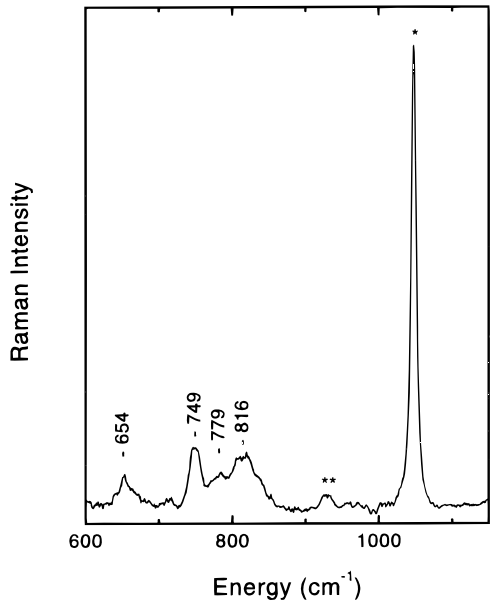

Figure 4. Resonance Raman spectra of the overtone/combination band region of *A. denitrificans* azurin excited at 568.2 nm. Peak at 1049 cm^{-1} (*) is from the nitrate internal standard. The marked feature (**) is a detector artifact. The spectrum is the sum of three scans.

The bands in this region have been assigned for *P. aeruginosa*[21] to a C−S fundamental mode at ∼750 cm^{-1} and various overtones and combination bands from the modes at 300−500 cm^{-1}. The assignment of these bands is expected to be similar for *A. denitrificans*. In analogy to *P. aeruginosa*, the peak at 749 cm^{-1} is probably due to the overlap of a fundamental band and a combination band. Because the resonance Raman spectra were taken at room temperature, we were unable to resolve the individual bands which had been observed in previous low-temperature resonance Raman spectra of *P. aeruginosa* azurin.[21] Table 2 lists the overall intensity of the overtone region from 774 to 875 cm^{-1}. These values were compared to the values calculated using eq 1 and the parameters in Table 2. The band at ∼750 cm^{-1} was not used due to the ambiguity in the assignment. The calculated overtone and combination band intensities agree with the experimental intensities within experimental error.

TABLE 2: Absolute Resonance Raman Cross Sections of the Overtone and Combination Bands of AD Azurin[a]

excitation wavelength (nm)	exptl cross section (Å²/molecule)[b]	calcd cross section (Å²/molecule)[c]
568.2	3.04×10^{-10}	2.85×10^{-10}
581.0	3.82×10^{-10}	3.90×10^{-10}
609.0	5.54×10^{-10}	5.19×10^{-10}
647.1	3.35×10^{-10}	3.94×10^{-10}

[a] The combination and overtone modes between 774 and 875 cm^{-1} were used. These modes are 774 (L+M), 787 (L+N), 798 (2M), 803 (L+O), 811 (M+N), 818 (L+P), 824 (2N), 827 (M+O), 835 (L+Q), 840 (N+O), 842 (M+P), 855 (N+P), 856 (2O), 859 (M+Q), 871 (O+P), and 872 (N+Q) cm^{-1}, in the notations of ref 21. [b] The resonance Raman spectra were measured at each wavelength using nitrate as an internal intensity standard. Cross sections were obtained from the intensities in the manner described in the text. [c] The cross sections were calculated with eq 1 using the parameters from Table 1.

Discussion

Electronic Structure. The resonance Raman intensities are sensitive to the electronic properties of the excited charge-

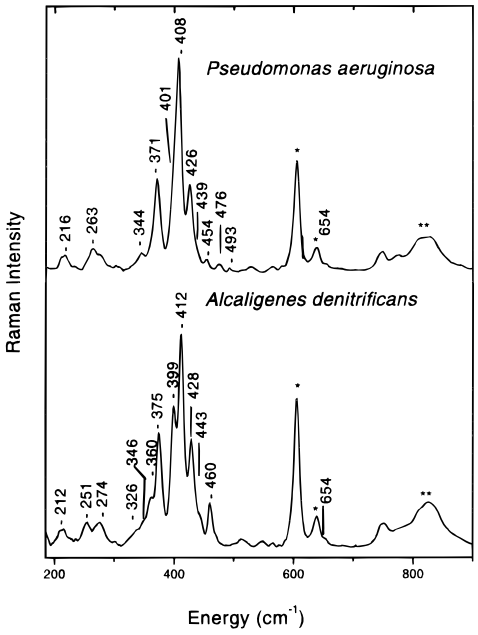

Figure 5. Comparison of resonance Raman spectra of *P. aeruginosa* (upper spectrum) and *A. denitrificans* (lower spectrum) azurins. Raman scattering of the internal intensity standard (cacodylate) is observed at 608 and 638 cm^{-1} (*). The broad band at ~820 cm^{-1} and the narrower band at ~750 cm^{-1} (**) are composed of the overtones and combinations of the azurin vibrations between 350 and 500 cm^{-1} and a cacodylate peak at 825 cm^{-1}. The spectra are the sum of three scans.

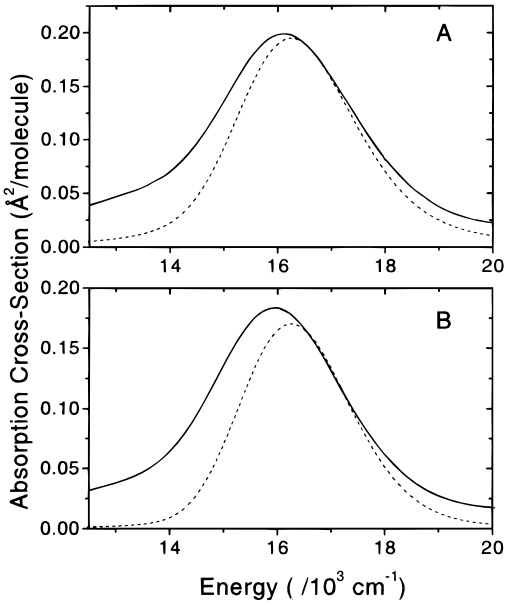

Figure 6. Experimental (—) and calculated (- - -) absorption spectra of azurin from *A. denitrificans* (A) and *P. aeruginosa* (B).

transfer state. The depolarization ratios and the overtone and combination band intensities were measured in an attempt to elucidate the electronic structure of this excited state. The depolarization ratios are found to be 0.41 for all of the modes across the absorption band. The lack of dispersion in the depolarization ratio and the similarity in the depolarization ratios of all of the modes argues that the observed Raman scattering arises from a single electronic transition. However, the mean depolarization ratio of 0.41 ± 0.05 is slightly higher than the value of 0.33 expected for totally symmetric modes on resonance and may indicate that the charge-transfer state is partially mixed with another electronic state.

As a further constraint on the parameters of the excited state, the overtone and combination band intensities were measured. A previous resonance Raman study of azurin, plastocyanin, and the multicopper oxidases laccase, ascorbate oxidase, and ceruloplasmin[21] has suggested that the high intensity of the overtone and combination bands between 700 and 900 cm^{-1} arises from different excited-state frequencies and/or Duschinsky rotation, a rotation of the ground-state normal modes in the excited electronic state. For the analysis performed here, it was not necessary to use Duschinsky rotation or changes of excited-state frequencies to obtain a self-consistent fit of the data.

Comparison of Azurins. The primary goal of this work is to model how the coordination geometry and protein environment modulate the excited-state properties of the copper center as probed by resonance Raman spectroscopy. A comparison of the results obtained from resonance Raman experiments on azurin from *A. denitrificans* (AD) and *P. aeruginosa* (PA), both of which have a known X-ray crystal structure, provides a unique opportunity to correlate differences in the observed resonance Raman spectrum and derived excited-state parameters with structure.

Figures 5 and 6 compare the resonance Raman and absorption spectra of azurin from *A. denitrificans* and *P. aeruginosa*. Table 1 lists the mode frequencies and mode-specific reorganization energies for both species. There are a number of similarities in the spectral properties of the two species. Many of the Raman frequencies are similar for the two species of azurin. The resonance Raman excitation profiles have similar shapes, reaching a maximum at the same energy. Self-consistent analysis of the absorption spectra and resonance Raman excitation profiles suggests the S → Cu charge-transfer transition occurs at a similar energy, even though the absorption band has a different λ_{max} in the two species. Finally, the two species have a similar total inner-sphere reorganization energy. All of these results suggest a similar nature of the charge-transfer process in the two azurins.

A closer inspection of the data in Figures 5 and 6, however, reveals some significant differences. There are differences in the frequencies for a few of the modes. For example, there are two overlapping modes at ca. 263 cm^{-1} for PA which are more well-resolved at 251 and 274 cm^{-1} in AD. PA has a weak mode at 344 cm^{-1}, while AD has a more intense mode at 360 cm^{-1} and a shoulder at 326 cm^{-1}. At higher frequencies, PA has several modes with low intensity (454, 476, and 493 cm^{-1}) which are not visible in AD. Rather, AD has a single medium-intensity mode at 460 cm^{-1} which is absent from PA. These differences indicate that the normal mode description of some of the modes are different for the two species. The relative intensities are also quite different for the two species, reflecting these changes in the normal mode description and/or indicating differences in the excited charge-transfer state.

A previous study has suggested that the mode with the greatest intensity is likely to have the greatest Cu−S stretching character and its frequency is an indicator of the Cu−S bond length.[7] The most intense modes are 412 cm^{-1} (AD) and 408 cm^{-1} (PA), while the X-ray crystal structures show that the bond lengths are 2.15 and 2.26 Å for AD and PA, respectively. The frequency of the most intense mode decreases as the bond length increases, which is expected. Due to the number of peaks in the resonance Raman spectra it is expected that the normal mode description of this vibration must contain other internal coordinates in addition to the Cu−S bond stretch.

As stated above, there are also differences in the absorption spectra. The experimental absorption band maximum changes from 16 000 to 16 155 cm^{-1} (625 to 619 nm) going from PA

to AD. However, analysis of the absorption spectra and the resonance Raman spectra (above) indicate that the S(Cys) → Cu charge-transfer transition has the same frequency for both AD and PA and is not blue-shifted in AD. The absorption bands, composed of ligand field and other charge-transfer transitions[27] in addition to the Cu(S charge-transfer transition, have been shown to be sensitive to the copper site coordination geometry,[7,23] which becomes slightly more tetrahedral on going from PA to AD. A survey of blue copper proteins does not reveal a clear relationship between the λ_{max} and the geometry of the copper site,[7,23] indicating that other electronic transitions within the absorption band influence λ_{max}. The change in copper coordination geometry can cause changes in the intensity of other electronic transitions by modulating the coupling between these transitions. In azurin there is a weak πS → Cu charge-transfer band at 526 nm[27] overlapping the πS → Cu charge-transfer transition in the ~620 nm band. An increase of the relative intensity of this band can shift the absorption band λ_{max} to the blue. The intensity of the πS → Cu charge-transfer band in three blue copper proteins increases in the order azurin < plastocyanin < stellacyanin,[27] corresponding to increasing tetrahedral geometry.[23] The more tetrahedral geometry of AD azurin is expected to lead to a blue-shift of the band as a result of increased dipole strength of the πS → Cu charge-transfer transition, and is what is observed. This change in coordination geometry to a more tetrahedral geometry should also result in an increase of the A_{470}/A_{620} intensity ratio[23] and that is what is seen (0.098 in AD vs 0.090 in PA).

Proposed Model. To determine the origin of these spectral differences, a comparison of the chromophore structure and protein environment was performed. The copper metal sits in an environment which can be divided into two components: the structural environment imposed by the protein and the electrostatic environment created by the protein. These two factors influence the properties of the excited charge-transfer state. A detailed examination of the spectra in Figure 5 and the Δ values in Table 2 can be useful in discriminating structural and electronic effects on the resonance Raman intensities. Table 2 shows that the total intensity of modes involving the Cu−N bond are larger in AD (212, 251, and 274 cm^{-1}) than those in PA (216 and 263 cm^{-1}). The combined intensity of the 401 and 408 cm^{-1} modes in PA is approximately the same as the combined intensity of the 399 and 412 cm^{-1} modes of AD within experimental error. Also, the intensity of the mode at 460 cm^{-1} in AD is roughly equal to the intensity of the 454, 476, and 493 cm^{-1} modes in PA. For the 401/408 cm^{-1} and the ca. 460 cm^{-1} modes, the resonance Raman intensity simply seems to be redistributed among vibrations with similar frequencies. However, the changes in the intensity in the Cu−N modes is much more dramatic, suggesting a larger perturbation of the vibrations by the structural and/or electrostatic differences between the two azurins.

To understand these intensity changes, a comparison of the structures was performed. Since the resonance Raman intensities are dependent on Δ, the difference between ground- and excited-state geometry along each normal mode, the properties of both the ground- and excited-state must be considered. The structure of the azurin molecule for *P. aeruginosa* and *A. denitrificans* can be compared by overlapping the protein backbone of the two species. Figure 7A shows a histogram of the RMS deviations for each residue and shows that most of the residues have a low RMS difference with a median value of 0.56 Å. In addition, the overall RMS deviation is 0.83 Å using 1026 atoms, indicating that the overall structures for the

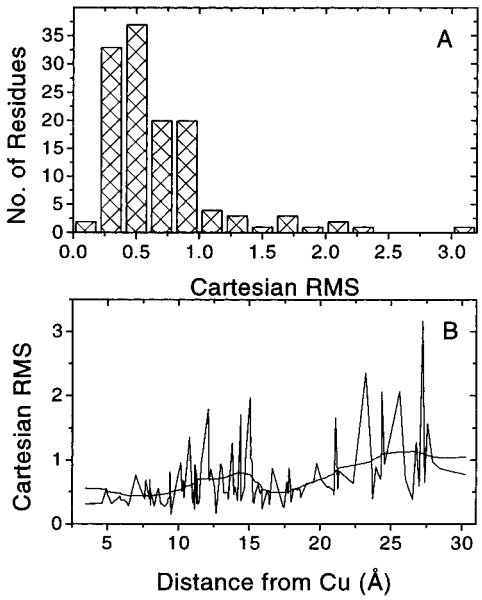

Figure 7. (A) RMS per residue histogram comparing structures of AD and PA azurin. (B) RMS per residue vs distance from the copper center. The distance of each residue was calculated using the α carbons only. The solid line through the plot is the same data after FFT filtering to show RMS trend with distance.

two species are similar. Figure 7B shows that the differences in structure tend to increase further from the copper site. However, a detailed comparison of the structure around the copper metal shows that it is somewhat different for the two proteins.[6,20] In AD the copper is slightly further above the NNS plane compared with PA. The copper moves further from Gly45 (3.13 vs 2.93 Å) and closer to Cys112 (2.15 Å vs 2.26 Å) in AD azurin. This results in a slightly more tetrahedral geometry of the copper site in AD azurin. These differences in the coordination geometry may change the normal mode descriptions. In a previous study of plastocyanin it was found that structural changes result in a redistribution of Raman intensity among two or more vibrational modes.[11] For AD and PA azurins, a similar mechanism may be operating because these two azurins differ much more substantially in the copper site structure than the two plastocyanins. These slight differences in the coordinating residue distances of the two azurins may change how the internal coordinates of cysteine couple to the S_γ−Cu stretch, resulting in a change in the normal mode description. These structural differences would be observed as a redistribution of Raman intensity among the vibrational modes between 320 and 500 cm^{-1} as seen for the 401/408 cm^{-1} bands and the ca. 460 cm^{-1} band.

Further support for this intensity redistribution comes from a comparison of the Raman spectra and X-ray crystal structures of the two species of azurin. The crystal structures suggest that the Cu−S(Cys) bond lengthens from 2.15 Å in AD azurin to 2.26 Å in PA azurin. Badger's rule[30] is an empirical relationship between the bond length and vibrational frequency, assuming no changes in the normal mode description, and can be used to calculate the expected frequency shift with bond length change. Using the Badger's rule relationship, $(r_1 - d)/(r_2 - d) = (\nu_2/\nu_1)^{2/3}$, with[7] $r_1 = 2.15$ Å, $r_2 = 2.26$ Å, $d = 1.5$, and $\nu_1 = 412$ cm^{-1} yields $\nu_2 = 325$ cm^{-1}, a downshift of 87 cm^{-1}. Only a 4 cm^{-1} downshift is observed, in the predicted direction, but with a very different magnitude. This serious deviation from Badger's rule supports intensity redistribution via an amino acid dependent rotation of the normal modes, as proposed earlier for the plastocyanins.[11]

The modes at 212, 251, and 274 cm^{-1} in AD azurin and at 216 and 263 cm^{-1} in PA azurin which involve the Cu−N bonds require further comment. There is a lack of conservation of resonance Raman intensity in these modes (Table 1); in AD azurin, the reorganization energy is 40% greater than in PA azurin. The higher intensity of Cu−N(His) modes in AD azurin may reflect a different electrostatic environment near the histidines. Changes in the electrostatic environment provide new repulsive or attractive forces which may result in a new equilibrium geometry of the excited state and a new excited-state displacement. Different vibrational modes may be affected differently and independently, depending on the relative positions of dipoles and charges within the two azurins. There are several changes in the electrostatic environment within 15 Å of the copper site. There are four amino acid changes which involve a change in charge on going from PA to AD: Gln8 changes to Glu, Asn16 changes to Asp, Ser34 changes to Lys, and Met56 changes to Lys. The first three are closest to His46 and may be the origin of the increased Raman intensity of the Cu−N modes in AD. The last change is closest to the Cys112 and may influence Cu−S modes. In addition to the charge changes, there are five dipole changes on going from PA to AD: Gly9 changes to Ser, Gln12 changes to Ala, Ser89 changes to Gly, Ser118 changes to Trp and Asn42 changes to Ser. The first three of these dipole changes are closest to His46, the fourth is closest to His117, and the fifth is closest to Gly45. Again, these changes are expected to have an overall greater effect on the Cu−N modes due to their proximity to the histidines. Work is in progress to further separate the contributions of the structural and electrostatic factors to the mode-specific excited-state dynamics.

Conclusions

Self-consistent analysis of the resonance Raman excitation profiles and absorption spectrum of AD azurin demonstrates that the azurins have an inner-sphere reorganization energy of 0.26 eV. A comparison of the results for PA and AD azurin indicate that the observed spectral changes are due to a complex relationship between chromophore structure and protein environment at the copper site. The most important factors affecting the excited-state properties of the copper site appear to be the immediate geometry and the electrostatic environment of the protein. In particular, the different frequencies and intensities observed in the resonance Raman spectra of the two azurins suggests the protein tunes the charge-transfer dynamics in these two azurins via structurally induced changes in the normal mode descriptions and selective distribution of charges and dipoles in the protein environment.

Acknowledgment. We thank T. D. Harris, M. Palcic and H. B. Dunford for equipment support and N. Scherer for providing a preprint of his work. We also thank R. Mah and M. Pickard at the University of Alberta for the growth and harvesting of *A. denitrificans*. Financial support was provided by NSERC and the Alberta Heritage Foundation for Medical Research.

Supporting Information Available: Table 3 listing the experimental and calculated absolute resonance Raman cross-sections and Figure 8 showing the resonance Raman spectra at each wavelength used in this study (3 pages). Ordering and access information is given on any current masthead page.

References and Notes

(1) Sykes, A. G. *Adv. Inorg. Chem.* **1991**, *36*, 377.
(2) Adman, E. T. *Adv. Protein Chem.* **1991**, *42*, 145.
(3) Hyun, Y.-L.; Davidson, V. L. *Biochemistry* **1995**, *34*, 12249.
(4) van Pouderoyen, G.; Cigna, G.; Rolli, G.; Cutruzzola, F.; Malatesta, F.; Silverstrini, M. C.; Brunori, M.; Canters, G. W. *Eur. J. Biochem.* **1997**, *247*, 322.
(5) Zumft, W. G.; Gotzmann, D. J.; Kroneck, P. M. H. *Eur. J. Biochem.* **1987**, *168*, 301.
(6) Baker, E. N. *J. Mol. Biol.* **1988**, *203*, 1071.
(7) Andrew, C. R.; Yeom, H.; Valentine, J. S.; Karlsson, B. G.; Bonander, N.; van Pouderoyen, G.; Canters, G. W.; Loehr, T. M.; Sanders-Loehr, J. *J. Am. Chem. Soc.* **1994**, *116*, 11489.
(8) Andrew, C. R.; Sanders-Loehr, J. *Acc. Chem. Res.* **1996**, *29*, 365.
(9) Han, J.; Adman, E. T.; Beppu, T.; Codd, R.; Freeman, H. C.; Huq, L.; Loehr, T. M.; Sanders-Loehr, J. *Biochemistry* **1991**, *30*, 10904.
(10) Fraga, E.; Webb, M. A.; Loppnow, G. R. *J. Phys. Chem.* **1996**, *100*, 3278.
(11) Loppnow, G. R.; Fraga, E. *J. Am. Chem. Soc.* **1997**, *119*, 896.
(12) Webb, M. A.; Kwong C. M.; Loppnow, G. L. *J. Phys. Chem. B* **1997**, *101*, 5062.
(13) St. Clair, C. S.; Ellis, W. R. J.; Gray, H. B. *Inorg. Chim. Acta* **1992**, *191*, 149.
(14) Albrecht, A. C.; Hutley, M. C. *J. Chem. Phys.* **1971**, *55*, 4438.
(15) Loppnow, G. R.; Mathies, R. A. *Biophys. J.* **1988**, *54*, 35.
(16) Ferraro, J. R.; Nakamoto, K. Introductory Raman Spectroscopy; Academic Press Inc.: San Diego, CA, 1994.
(17) Myers, A. B.; Mathies, R. A. In *Biological Applications of Raman Spectroscopy*; Spiro, T. G., Ed.; Wiley: New York, 1988; Vol. 2, p 1.
(18) Lee, S.-Y.; Heller, E. J. *J. Chem. Phys.* **1979**, *71*, 4777.
(19) Bernstein, F. C.; Koetzle, T. F.; Williams, G. J. B.; Meyer, E. F., Jr.; Brice, M. D.; Rodgers, J. R.; Kennard, O.; Shimanouchi, T.; Tasumi, M. *J. Mol. Biol.* **1977**, *112*, 535.
(20) Nar, H.; Messerschmidt, A.; Huber, R.; van de Kamp, M.; Canters, G. W. *J. Mol. Biol.* **1991**, *221*, 765.
(21) Blair, D. F.; Campbell, G. W.; Schoonover, J. R.; Chan, S. I.; Gray, H. B.; Malmstrom, B. G.; Pecht, I.; Swanson, B. I.; Woodruff, W. H.; Cho, W. K.; English, A. M.; Fry, H. A.; Lum, V.; Norton, K. A. *J. Am. Chem. Soc.* **1985**, *107*, 5755.
(22) Dave, B. C.; Germanas, J. P.; Czernuszewicz, R. S. *J. Am. Chem. Soc.* **1993**, *115*, 12175.
(23) Han, J.; Loehr, T. M.; Lu, Y.; Valentine, J. S.; Averill, B. A.; Sanders-Loehr, J. *J. Am. Chem. Soc.* **1993**, *115*, 4256.
(24) Qiu, D.; Dong, S.; Ybe, J. A.; Hecht, M. H.; Spiro, T. G. *J. Am. Chem. Soc.* **1995**, *117*, 6443.
(25) Grundler, H.; Schumann, H. D.; Steger, E. *J. Mol. Struct.* **1974**, *21*, 149.
(26) Vansant, F. K.; van der Veken, B. J.; Herman, M. A. *Spectrochim. Acta* **1974**, *30A*, 69.
(27) Solomon, E. I.; Hare, J. W.; Dooley, D. M.; Dawson, J. H.; Stephens, P. J.; Gray, H. B. *J. Am. Chem. Soc.* **1980**, *102*, 168.
(28) Hemley, R. J.; Dawson, J. I.; Vaida, V. *J. Chem. Phys.* **1983**, *78*, 2915.
(29) Morris, D. E.; Woodruff, W. H. *J. Phys. Chem.* **1985**, *89*, 5795.
(30) Herschbach, D. R.; Laurie, V. W. *J. Chem. Phys.* **1961**, *35*, 458.